NaSTech JOURNAL OF NATURAL SCIENCES AND TECHNOLOGIES
2023, 2(2), pp. 195-208, DOI: 10.5281/zenodo.8103391

MANUFACTURING AND CHARACTERIZATION OF ALUMINUM BASED POROUS MATERIALS: PHYSICAL PROPERTIES AND MECHANICAL BEHAVIOR

Ali Dinçer OGAN

Tribology Laboratory, Dept. of Mechanical Engineering, Erciyes University, Kayseri, TURKEY
Department of Materials Science and Engineering, Anadolu University, Eskişehir, TURKEY

ABSTRACT

Porous aluminum samples were manufactured by powder metallurgy method. In the powder metallurgy method, pure Al 99 % powder (< 44μm) and TiH_2 powder of two different sizes (< 44 μm and 1-3 μm) were mixed at different volume fractions. All the porous samples were subjected to a compression test and characterized by electrical conductivity, hardness and specific heat capacity measurements according to the porosity observed by image analysis. It was determined that compression strength is decreased by the percentage of total pore area in the section. The specific heat capacity values of the porous material are increased slowly by TiH_2 size, pore number and pore area. The electrical conductivity of the porous material has a decreasing trend dependent on the percentage of TiH_2.

Keywords: porous aluminum material, blowing agent (TiH_2), pore characteristics, compression strength

1. INTRODUCTION

Porous metals represent a new class of materials with extremely low densities and a unique combination of excellent mechanical, thermal, electrical and acoustic properties. Because of these properties, they are commonly preferred for use in a wide range of applications in industrial sectors, such as the automotive, aerospace and construction industries. Many researchers have aimed to obtain a metallic structure with porosity through the use of powder metallurgy or casting processes. In the manufacturing of Al-based porous material, A 356, 1060, 3003, 6016 or 6061 Al materials are widely utilized in powder or bulk forms. Cast Al-Si alloys are also frequently used because of their low melting points and good foaming properties as described by Chin et al. (1998) [3]. With the addition of appropriate amounts of porosity forming agents, powder or bulk aluminum can be used for constructing porous aluminum as also shown in this study.

Porous Al materials or metallic foams can be obtained by various manufacturing routes as previously reported by John (2000) [9]. Some of these routes are already in use as commercial manufacturing methods for the production of Al-based foams, such as gas injection into molten Al material and the addition of blowing agents into molten aluminum in his research. Different blowing agents, such as $CaCO_3$, $CaAl_2O_4$ and Al_4Ca, were added into molten aluminum by Chen et al. (1999) [2]. and Luis et al. (2009) [12]. In the powder metallurgy technique, blowing powders are mixed homogeneously with the Al powders and compressed. For instance, powder agents like TiH_2 produce blowing gas in the matrix of Al powders as recently studied by Masanori et al. (2010) [13]. Alternatively, Ken et al. (2010) [10]. produced aluminum foam with a relative density of 0.27 using two repeats of backward extrusion and cup compression. In their study, 1.5%wt. TiH_2 and 4%wt. silicon powder were used as the blowing agents. Ken et al [10]., however, did not try to increase the volume fraction of TiH_2 in their research.

The researchers generally followed the above-mentioned manufacturing routes. In the present study, all-in-one benchmarking of the manufacturing routes was done through mechanical tests and physical examinations. The present work also expands the volume fraction of the blowing agent TiH_2 in aluminum, and discusses its effects on porosity occurrences using different manufacturing techniques.

Porous materials are characterized structurally by their pore topography, relative density and pore size. Hans and Brigitte (2002) reported that the mean size of pores and relative density were effective parameters for the thermal and mechanical properties of the porous materials [8]. However, in their work, quantity of pores and total pore area per solid volume were not taken into account, nor were their effects on thermal and mechanical properties of aluminum porous materials discussed. Remy et al. (2009) [14]. also structurally characterized a metallic part from standard trade-mark foam. However, we investigated pore characteristics associated with three different manufacturing methods at laboratory scale. Experimental data in the present study are interested in these properties of porous aluminum materials.

Many porous materials have both closed and open cells as described by Lorna and Michael (1997) [11]. These types of cells greatly affect the mechanical properties of porous aluminum materials. Experimental studies by Anthony et al. (1998) have shown that the mechanical behaviors of porous materials with open and/or closed cells are very different [1]. Douglas et al. (2004) pointed out that porous materials with closed cells had more strength for load-carrying rigidity and impact [5]. Additionally, Enrique and Carlo (2009) produced Cu-based and

interconnected open-cell foams with spherical cell morphology by the infiltration method [6]. The authors elaborated production process parameters, relative density and compressive stress-strain behavior in their study.

The conclusions inferred from the above four works indicated that closed cells increased the compression strength of porous material although they reduced the rigidity of the material.
In this work, we focused on structures with open cells and also revealed the reinforcement effects of blowing agents, which stayed in the bulk without forming any open and/or closed cells.

The uni-axial compressive and tensile modulus and strength of several aluminum foams were compared with the finite element model for cellular solids by Erik et al. (1999) [7]. However, they examined only the compressive and tensile examinations of aluminum foams made by industrial manufacturers. Doretea et al. (2006) also worked on the formability of aluminum foam sandwiches through experiments and numerical simulations of commercially prepared panels unlike those that were done in the present study. In both studies, unlike the present study, the researchers did not manufactured porous aluminum samples [4].

Thilo et al. (2001) carried out a study in which axial compression tests were performed at different aluminum circular and rectangular hollow structures that are partially and completely filled with aluminum foam [15]. The compressive force-strain curves with their corresponding buckling mode and the absorbed energy were compared. However, in the work by Thilo et al. (2001), the researchers didn't take into account pore characteristics when discussing the absorbing energy at maximum load [15]. In the present work, variation in the absorbed energy has been evaluated according to the parameters of the porosity forming processes. The purpose of the study is to manufacture porous aluminum samples by gas injection, blowing agents and powder metallurgy, and to characterize their compression, hardness, electrical and specific thermal properties depending on the porosity.

2. MATERIAL METHODS

The chemical compositions of aluminum materials in this study are given in Table 1. Due to its wide usage in the aerospace industry, Al 99 was used as the test material for the manufacture of porous material using.

In the powder metallurgy method, pure Al powders (Al 99) < 44 μm were used as the matrix material; TiH_2< 44 μm and TiH_2 powders with particles 1-3 μm in size were used separately as the porosity former material. The metal powders were mixed mechanically by using 5 mm diameter zirconium balls for 1.5 hours. The volume fractions of the TiH_2 powders of two different sizes in the Al powders were as follows: 0.6, 1, 10, 15, 20, 25, 30, 40 and 50%wt. After mixing, the composite powders were put into a steel die and pressed under 400 MPa. Many of the samples prepared with different volume fractions of TiH_2 were sintered at 750ºC for 75 and 90 minutes to obtain porosities in the melted Al matrix material. The sample preparation procedure in this technique is given in Figure 1.

Table 1. Chemical compositions of the aluminum materials

Material	Elements %							
	Al	Cu	Fe	Mg	Mn	Si	Cr	Zn
Al 99	99.2	-	-	-	-	-	-	-

Some of samples obtained by the method mentioned above were sectioned, polished and etched for metallographic examinations. Optical and SEM examinations, hardness measurements such as HB under 500N and image analysis were applied to determine their microstructure, porosity distribution and size, and density. The microstructures of the samples were also analyzed by the EDX method for element determination. The electrical and specific heat capacity measurements were also carried out from a characterization point of view. All samples were subjected to compression tests by an Instron compression tester to determine the mechanical properties of the samples. The effects of porosity on compression strength, hardness, electrical and specific heat capacity were characterized, and the effects of manufacturing method on pore size and area rate in the matrix were also examined.

2023, 2(2), pp. 195-208, DOI: 10.5281/zenodo.8103391

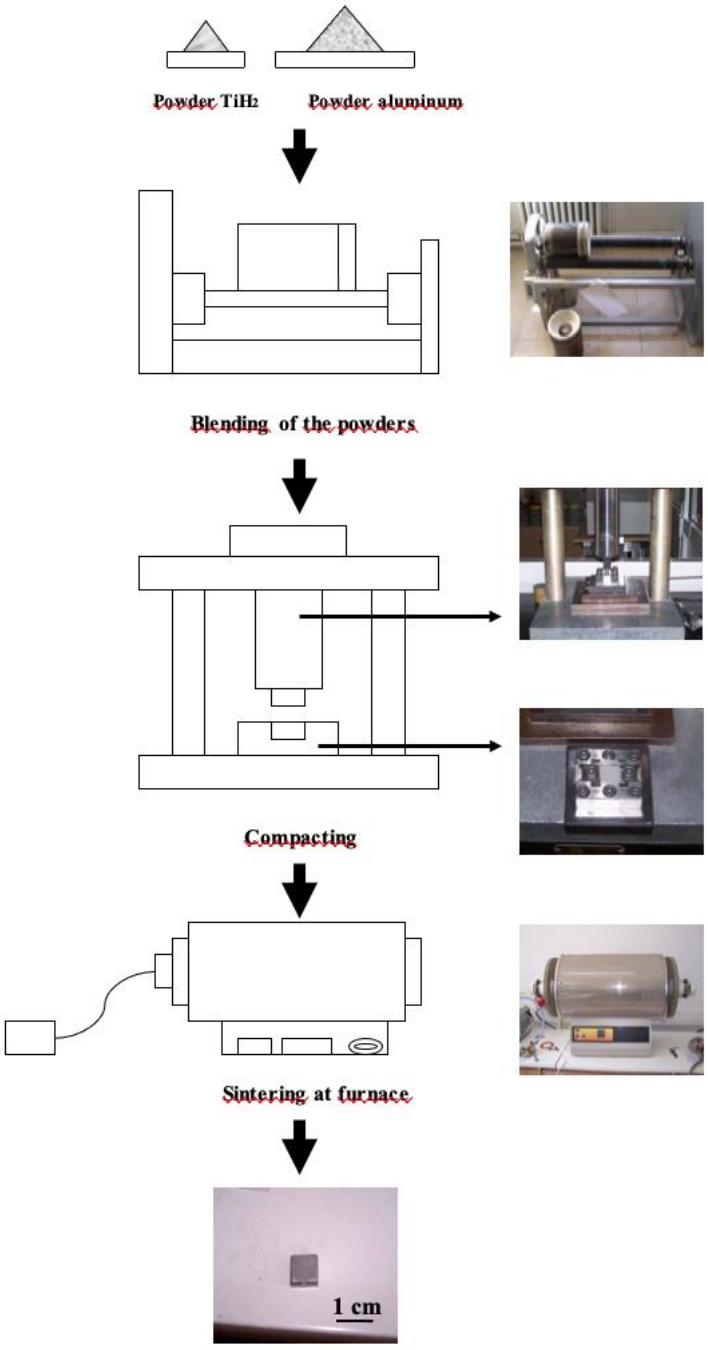

Figure 1. Schematic illustration of the manufacturing processes

3. RESULTS AND DISCUSSION

The pores in several samples manufactured by powder metallurgy techniques by the mixing of Al and TiH_2 powders were obtained during the sintering of the material at 750°C. Pores can start to form with the decomposition of TiH_2 at 465°C. The higher the sintering temperature, the more gas was produced from the TiH_2 in the matrix. On the other hand, it was observed in pre-tests that when the sintering temperature rose to 880°C, sizeable cracks on the surface resulted (Fig.2). Therefore, the maximum sintering temperature was determined as 750°C for 60 min.

NaSTech
JOURNAL OF NATURAL SCIENCES AND TECHNOLOGIES
2023, 2(2), pp. 195-208, DOI: 10.5281/zenodo.8103391

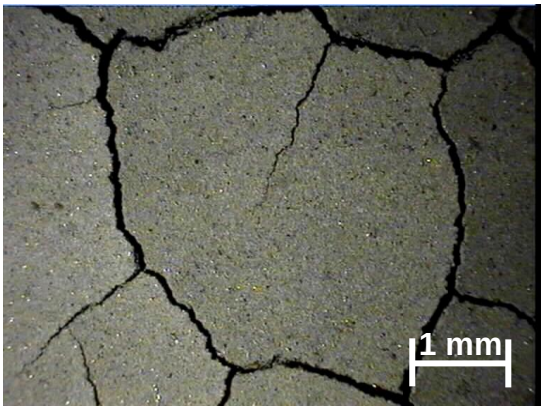

Figure 2. Cracks on the surface resulted from sintering at 880°C

The powders and the mixing conditions can be seen in Table 2.

Table 2. The numbered list of samples prepared from aluminum and TiH_2 powders

Volume fraction	**Al (< 44 µm)**	
	TiH_2 (< 44 µm)	**TiH_2 (1-3 µm)**
% 0.6	34, 36*, 40	**19, 20, 22, 24, 25, 27,28*,29**
% 1	23, 26, 35, 37, 41*	**33, 38*, 39**
% 10	1	
% 15	11, 18, 31	
% 20	2, 13, 15, 16, 17	
% 25	12, 30	
% 30	3, 6, 7, 8, 32	
% 40	4, 14	
% 50	5	
*** The unsintered samples**		

The porous microstructure obtained by gas production during sintering can be seen in Figure 3a. It is understood from the figure that pore distribution is not homogenous, but is at a sufficient level to be classed as porous.

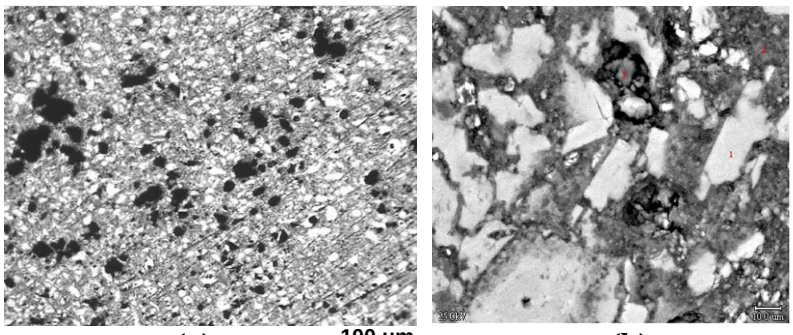

(a) **(b)**

Figure 3. Microstructure of sample 13
a) at low magnification **b)** at high magnification

In Figure 3b, there are three different colored areas. The gray, dark and white areas are Al, pores and Ti respectively. The pore-pits include oxygen, aluminum and titanium in different percentages. When comparing tables 3 and 4, it can be seen that the percentage of total pore areas was increased by the volume fraction of TiH_2 (samples 23 and 34). On the other hand, the volume fraction of TiH_2 particles with a constant size decreases the pore diameters under non-sintering conditions; increasing TiH_2 particle size with a 0.6% volume fraction slightly increases the percentage and average diameter of the pores (samples 28 and 36).

Table 3. The results of image analyses with respect to the numbered samples

	Sample No.										
	19	**22**	**23**	**24**	**25**	**27**	**28**	**33**	**34**	**35**	**36**
Pore area fraction (%)	0.51	1.63	47.73	8.15	0.50	0.25	16.66	0.66	30.14	2.11	**20.36**
Average diameter of pore (µm)	5.22	5.00	4.67	8.25	6.18	5.20	5.58	5.33	5.59	5.86	**5.75**
Max. diameter of pore (µm)	**6.83**	**6.64**	**6.26**	**12.00**	**7.83**	**6.76**	**7.19**	**7.11**	**7.57**	**5.89**	**7.42**

Samples 34 and 36 should be compared to understand the effects of the sintering process on the porosity of materials. While the unsintered sample 36 has a total pore area of 20.36%, the sintered sample 34 has an area of 30.14%. On the other hand, the average pore diameter is slightly reduced by the sintering process (i.e. 5.75 µm to 5.59 µm). It can be seen that the particle size of the TiH_2 in the Al matrix increases the percentage of the pore area on the sample surface while an increase in the volume fraction of TiH_2 reduces the pore areas (Fig. 4).

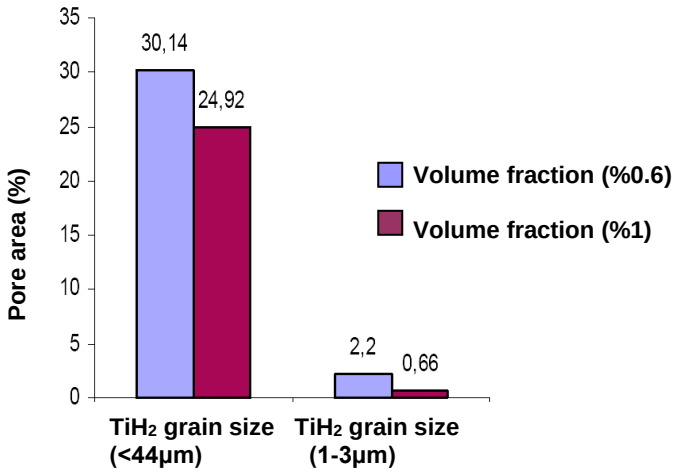

Figure 4. Effect of particle size and volume fraction of TiH_2 on the percentage of pore area

As for electrical properties, the measured electrical conductivities of all the samples have different values and there is no systematic relationship depending on pore size and area. On the other hand, it was determined that the electrical conductivity of the porous samples is lower than those of some Al alloys. While the measured average electrical conductivity value of the samples in this study is 17.86 IACS (International Annealed Copper Standard), those of some Al alloys are very high at approximately twice that of the samples. (i.e. above 40 IACS) (Fig.5). It is well known that this is caused by transitory factors such as pores, oxides, etc.

2023, 2(2), pp. 195-208, DOI: 10.5281/zenodo.8103391

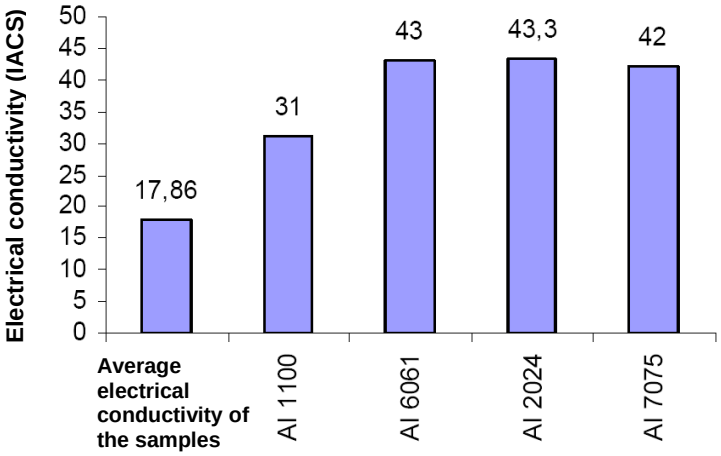

Figure 5. Comparison of the electrical conductivity of the porous samples manufactured by powder metallurgy with the other Al alloys

The specific heat capacity (C_p) values of the porous samples were measured and it was observed that they are close to each other at between 0.141-0.204. The average value of all samples is 0.169 J/g ^oC. When the specific heat capacities of the samples were compared with pure Al (i.e. 0.92 J/g ^oC), it was understood that the pores reduce the specific heat capacity of the aluminum material. These properties, like electrical conductivity, were strongly related to the density of the material. As the pores caused a decrease in material density by keeping air or gas in their volume, the specific heat capacity values were generally increased with pore number and pore area.

The variation in specific heat capacity value with the percentage of total pore area on the material surface can be seen in Figure 6. Hence, this increase was very slow according to the increase in the percentage of pore area.

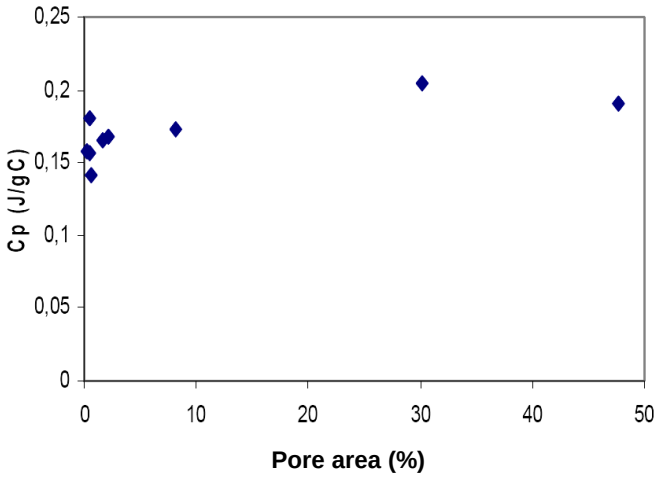

Figure 6. Variation of specific heat value of porous sample with percentage of total pore area

The compression tests conducted on some porous samples manufactured by the powder metallurgy method show that the samples have a yield strength between 80-100 MPa. After the yielding points, some samples broke in the sections with more numerous or large pores (Sample nos. 3, 4 and 7). For example, the compression test curves of the sintered sample 37 and unsintered one, sample 38, can be seen in Figures 7a and b. While the sintered sample shows yielding at a stress of 68.44 MPa, the maximum compression stress of the sample is nearly 230 MPa with 45% strain. The Young's modulus of the sintered sample was determined as 3.31 GPa (Fig.7a).

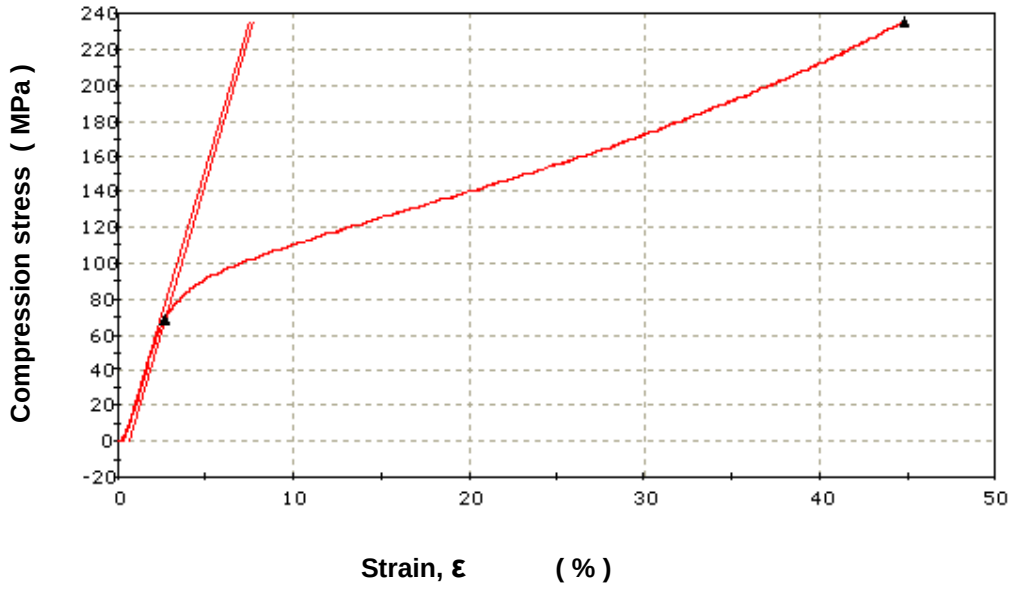

(a)

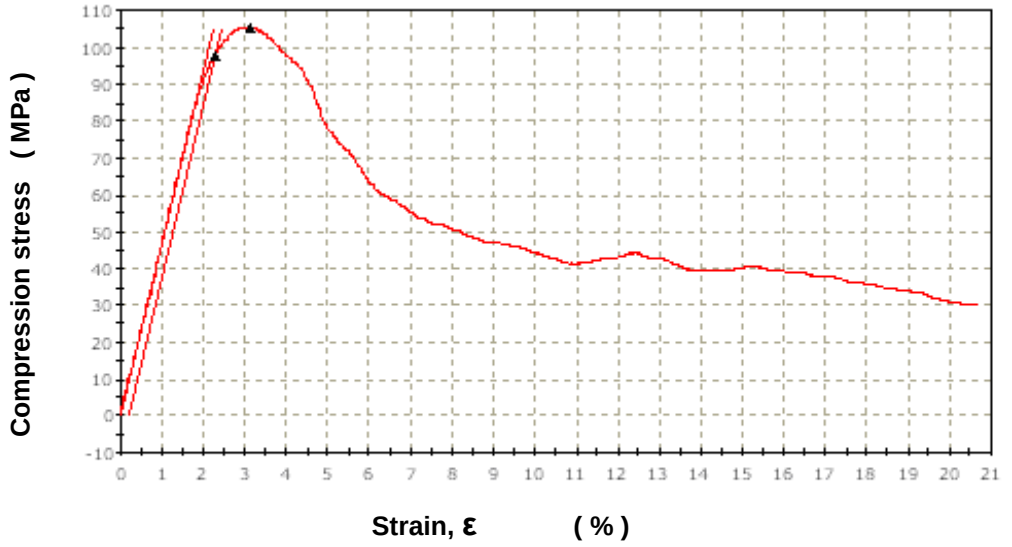

(b)

Figure 7. Compression test results of sintered and unsintered samples
- **a)** sample 37 (sintered)
- **b)** sample 38 (un-sintered)

On the other hand, the un-sintered sample 38 has higher yielding and lower ultimate stresses than those of the sintered sample at 97.92 and 105 MPa respectively. This sample has also a Young's modulus of 4.74 GPa. (Fig.7b). For samples 37 and 38, it was determined that the energies absorbed at the maximum compression loads are 124.04 and 3.2 Joules, respectively. This comparison shows that the sample with a higher percentage of total pore area is tougher than the others.

NaSTech
JOURNAL OF NATURAL SCIENCES AND TECHNOLOGIES
2023, 2(2), pp. 195-208, DOI: 10.5281/zenodo.8103391

The effect of volume fraction and size of TiH_2 particles on the compression properties of the porous material manufactured by the powder metallurgy method can be seen in the next figures. It can be observed from Figure 8. that the compression strength, Young's modulus and absorbing energy of the material with TiH_2 with a particle size of 1-3 μm during the compression test are higher than those of the material with TiH_2 with a particle size of <44 μm in the case of 0.6% and 1% volume fractions.

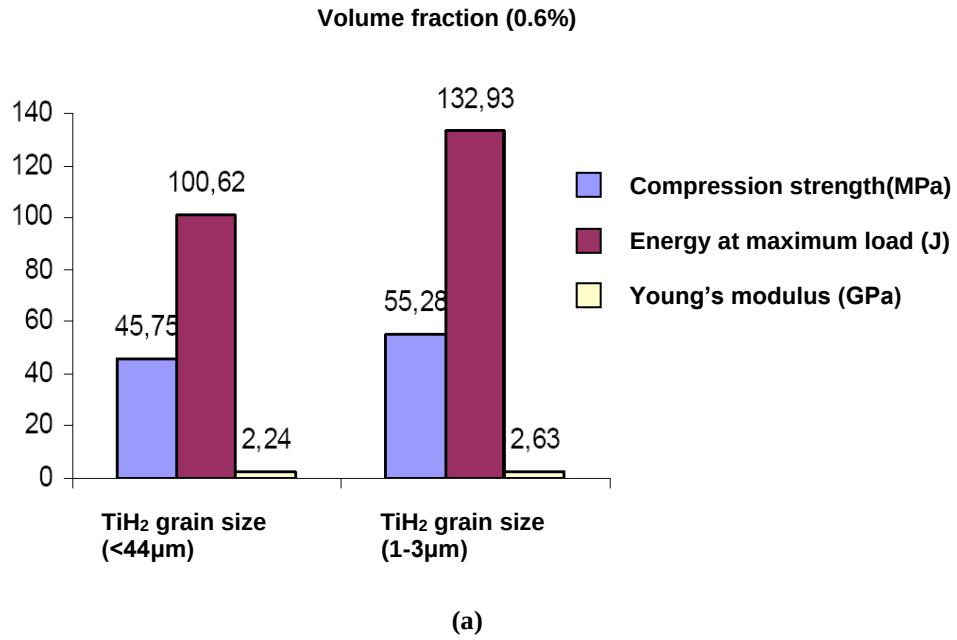

(a)

Figure 8. Effect of TiH_2 particle size on the compression properties of the porous material. The compression test data obtained from the porous materials manufactured using TiH_2 volume fractions of different sizes

a) 0.6% TiH_2 volume fraction

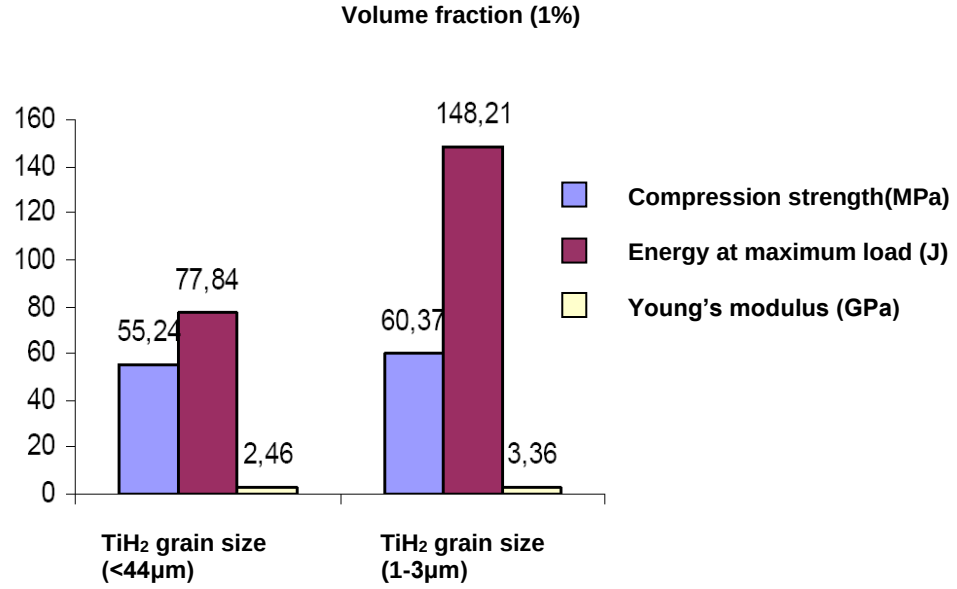

(b)

Figure 8. Effect of TiH_2 particle size on the compression properties of the porous material. The compression test data obtained from the porous materials manufactured using TiH_2 volume fractions of different sizes

b) 1%TiH_2 volume fraction

This demonstrates that fine TiH_2 particles produce fine pores in the material matrix which is stronger than the material with coarse pores. It is surprising that the energy absorbed under maximum compression load was reduced by the volume fraction of TiH_2 with the same particle size (i.e. < 44 μm). This may be because of the increasing pore number; more particles can produce more pores. The variation of compression strength and absorbed energy with volume fraction of TiH_2 with a particle size of < 44 μm can be seen in Figures 9a and b, respectively. It can be seen from Fig. 9a that the average compression strength of the porous samples was increased by the volume fraction of TiH_2. This is because, while some of TiH_2 particles can produce gas in the matrix, some of them stay in the matrix as reinforcing particles. Therefore, the matrix has not only porous but also reinforced Ti particles. For this reason the matrix strength is increased by increasing the Ti volume fraction. While the matrix gained more compression strength with increased the volume fraction, it also lost some of its toughness. Therefore the energy absorbed during the compression test was reduced by TiH_2 volume fraction (Fig. 9b).

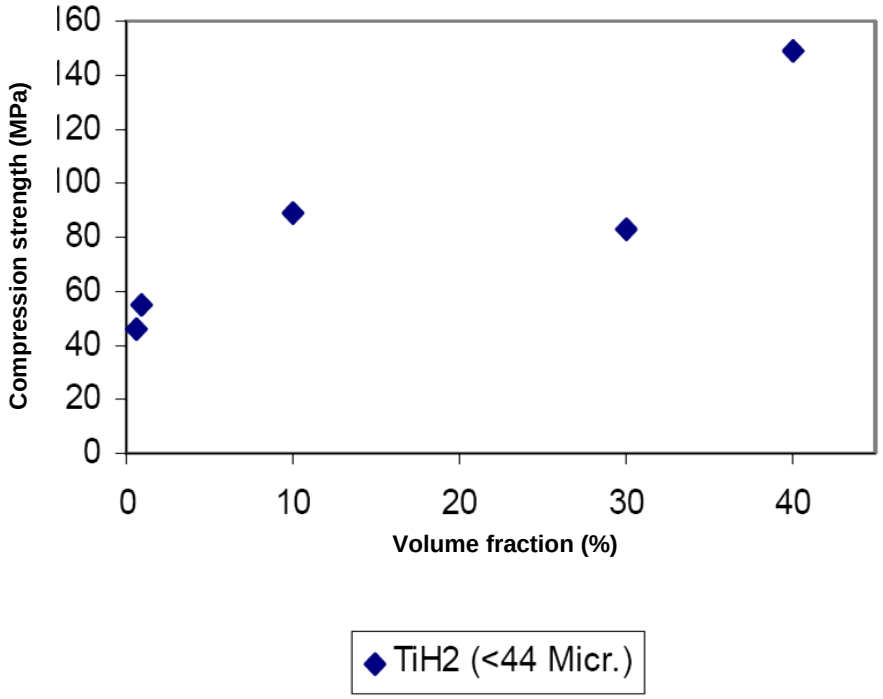

(a)

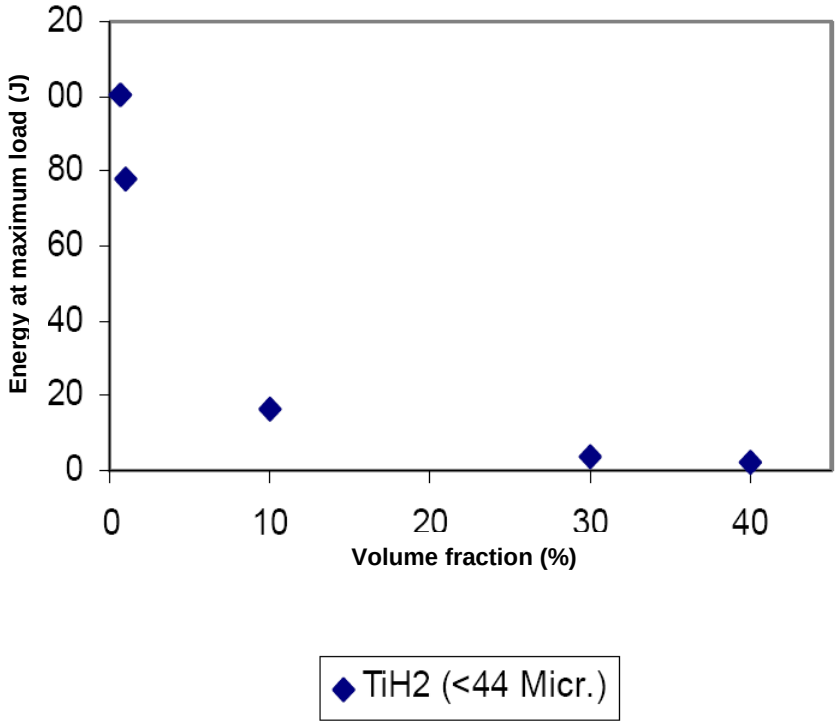

(b)

Fig.9. The effects of volume fraction of TiH_2 with a size of < 44 μm on
a) compression strength
b) absorbed energy at maximum compression load

Another cause of the decrease in absorbed energy and increase in compression strength in the porous material is the percentage of total pore area on the surface because the percentage of total pore area on the surface is decreased by the volume fraction of TiH_2 (Fig. 4). Due to the causes mentioned above, while the compression strength of porous material is increased by the volume fraction of the pore forming element TiH_2, the toughness of the material is reduced. This contrast can be also seen in Figure 10. At the same time, the increase in the volume fraction of TiH_2 increased the Young's modulus of the material by up to 30% TiH_2, then decreased, but to a value higher than 10% TiH_2 (Fig. 11).

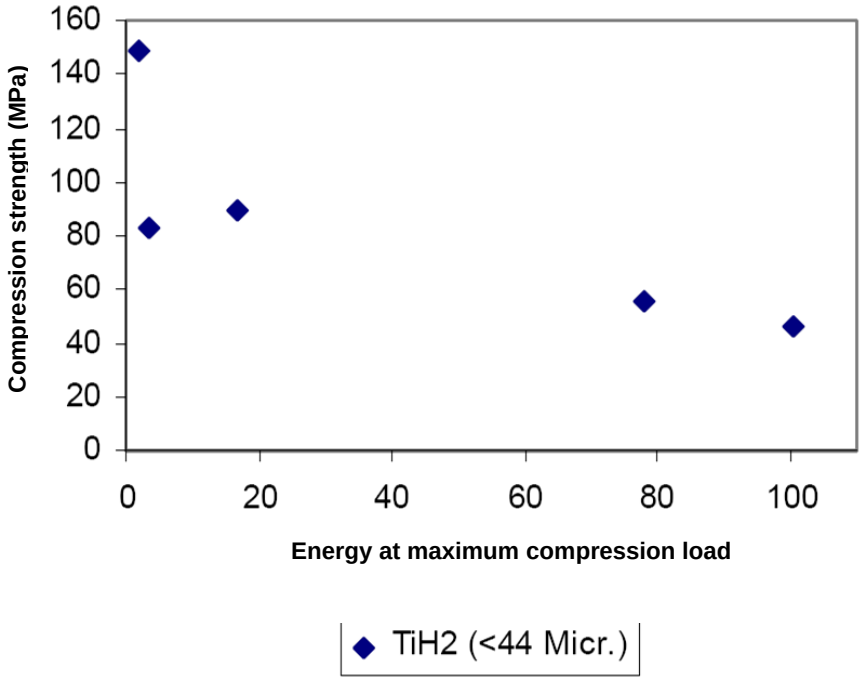

Figure 10. Variation of compression strength of the porous material with the absorbed energy

Young' s modulus (GPa)

2023, 2(2), pp. 195-208, DOI: 10.5281/zenodo.8103391

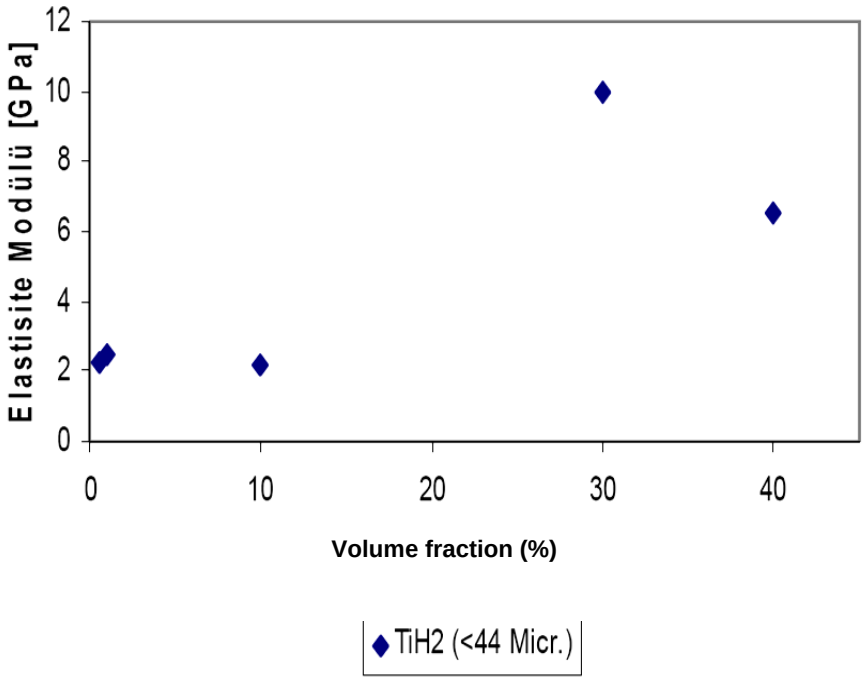

Figure 11. The effect of volume fraction of TiH_2 on the Young's modulus of the material

It is interesting that unsintered samples had more compression strength than sintered ones (Figs. 12a, b and c).

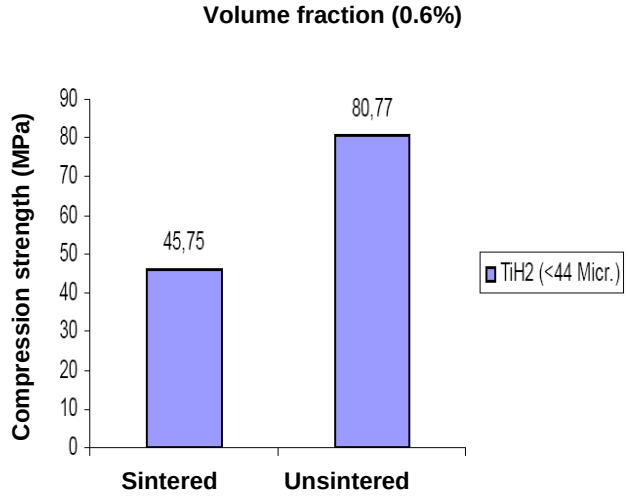

(a)

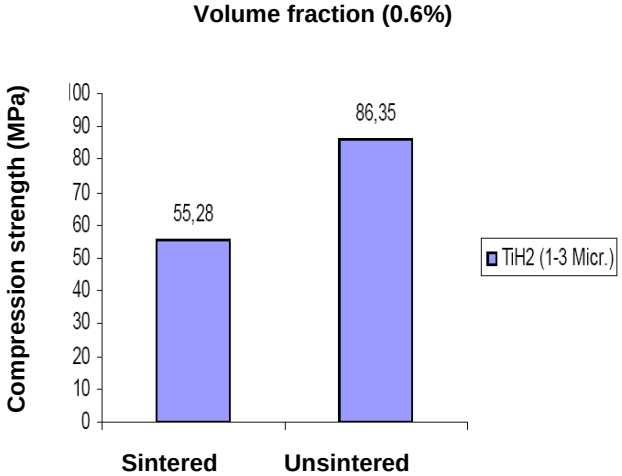

(b)

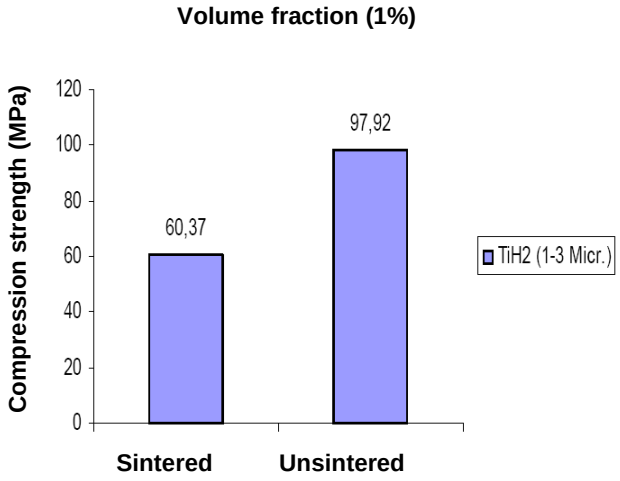

(c)

Figure 12. Comparison of compression strengths of sintered and unsintered material manufactured by different volume fractions and sizes of TiH_2

a) 0.6% volume fraction and TiH_2 particle size of < 44μm
b) 0.6% volume fraction of TiH_2 with particle size of 1-3 μm
c) 1% volume fraction of TiH_2 with particle size of 1-3 μm

This is because porosity was produced mainly during the sintering process. On the other hand, unsintered samples had pores which were produced by TiH_2 apart from other porosity caused by the nature of the powder metallurgy method itself. Therefore the pores were more numerous and coarser in material sintered with TiH_2 than in those which were not sintered. That is why the compression strengths of sintered samples with more numerous and coarser pores were lower than those of unsintered samples.

In contrast, the energy absorbed during the compression tests was higher for sintered samples than for unsintered ones (Figs. 13a and b). The more pores there were, the more energy absorption occurred due to the greater toughness caused by porosity. Parallel to this, the higher the porosity was, the lower compression strength was for porous matrix composites.

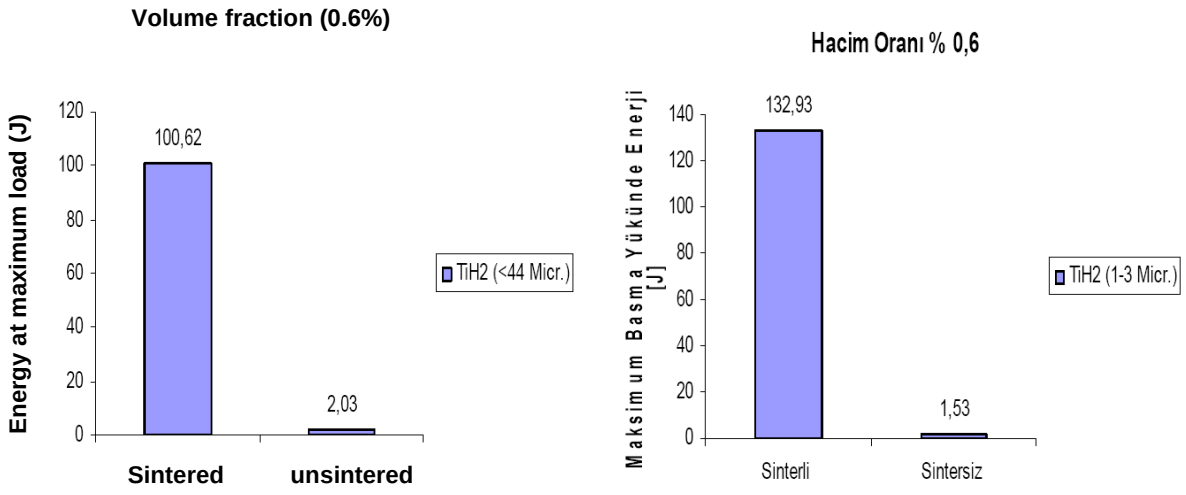

(a)

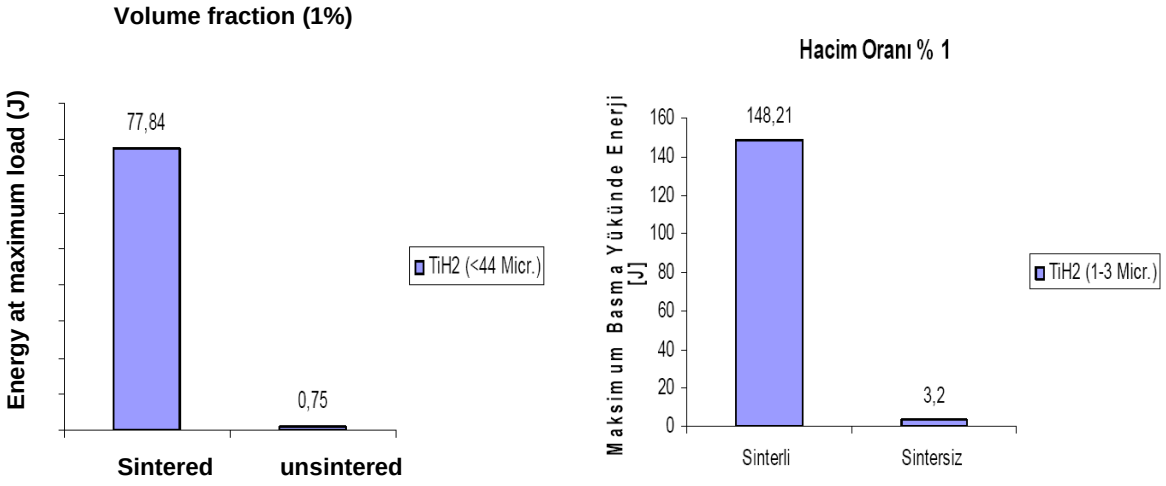

(b)

Figure 13. Variation of absorbed energy during maximum compression load for unsintered and sintered samples

a) with 0.6 % TiH_2

b) with 1 % TiH_2

4. CONCLUSIONS

The conclusions derived from this study can be summarized as follows:

1. In the manufacturing of porous materials by mixing Al and TiH_2 powders via the powder metallurgy method, the percentage of total pore areas is increased by the volume fraction of TiH_2 powders with a constant size. On the other hand, the average pore diameter is decreased by the volume fraction of TiH_2.
2. The particle size of TiH_2 in the Al matrix increases the percentage of pore area in the section while the pore areas are decreased by the volume fraction of TiH_2.
3. The electrical conductivity of the Al+TiH_2 composite material does not show a systematic relationship between pore size and area, and it is nearly 2 times lower than that of other Al alloys (i.e. Al 7075). The specific heat capacity values of the material are increased slowly by TiH_2 size, pore number and pore area.
4. The compression strength, Young's module and energy absorbing capacity of the porous material manufactured by TiH_2 with a particle size of 1-3 μm are higher than those of material with TiH_2 particles with a size of 44 μm because fine TiH_2 particles produce fine pores in the material matrix and the material is stronger than materials with coarse pores.
5. The compression strengths of the porous material is increased by volume fraction of TiH_2 but it decreases the toughness of the material.
6. The compression strengths of sintered finer porous material are lower than those of unsintered ones because sintered material has more numerous and coarser pores.

5. ACKNOWLEDGEMENTS

This manuscript was derived from the Ph.D. study of Ali Dinçer OGAN which was financially supported by the Scientific Research Project Council of Erciyes University (Grant No: FBT-07-78). The authors would like to thank the Department of Materials Science and Engineering, Anadolu University, Eskişehir, Turkey.

REFERENCES

[1] Anthony, G. E., John, W. H., Michael, F. A., 1998. Cellular metals, Curr. Opin. Solid St. M. 3, 288-302.

[2] Chen, F., He, DP., 1999. Metal foams and porous metal structures. In: Banhart J, Ashby M.F, Fleck NA, (Eds.). Int. Conference, Bremen, Germany, 14-16 June, MIT Press-Verlag p.163.

[3] Chin, Y., Harald, H. E., John, B., Joachim, B., 1998. Metal foaming by a powder metallurgy method: Production, properties and applications, Mater. Res. Innov. 2, 181-188.

[4] Doretea, C., Luigino, F., Livan, F., Fabrizio M., 2006. Forming of aluminum foam sandwich panels: Numerical simulations and experimental tests, J. Mater. Process. Technol. 177, 364-367.

[5] Douglas, T. Q., Yosuke, K., Haydn, N.G.W., 2004. Synthesis of stochastic open cell Ni-based foams, Synthesis of stochastic open cell Ni-based foams, Scripta Mater. 50, 313–317.

2023, 2(2), pp. 195-208, DOI: 10.5281/zenodo.8103391

[6] Enrique, M.C., Carlo, M., 2009. Processing of brass open-cell foam by silica-gel beads replication, J. Mater. Process. Technol. 209, 4958-4962.

[7] Erik, A., Wiebke, S., Lorna, J.G., 1999. Compressive and tensile behaviour of aluminum foams, Mat. Sci. Eng. A-Struct. 270, 113-124.

[8] Hans, P. D., Brigitte, K., 2002. Handbook of Cellular Metals, Production, Processing and Applications, Wiley-VCH, ISBN 3-527-29320-5.

[9] John, B., 2000. Manufacturing routes for metallic foams, JOM Journal of the Minerals, Metals and Materials Society, 52, 12, 22-27.

[10] Ken-ichiro, M., Hikaru, N., 2010. Cold repeated forming of compact for aluminium foam, J. Mater. Process. Technol. 210, 1580-1586.

[11] Lorna, J. G., Michael, F. A., 1997. Cellular Solids, Second Ed., Cambridge Solid State Science Series, ISBN 0-521-49560-1.

[12] Luis, E.G.C, Ruiz, R., Corpas, F.A, Ruiz, P., 2009. Manufacturing of Al-Mg-Si alloy foam using calcium carbonate as foaming agent, J. Mater. Process. Technol. 209, 1803-1809.

[13] Masanori, S. I., Kozo, O., Ryo, M., 2010. Fabrication of aluminium foams from powder by hot extrusion and foaming, J. Mater. Process. Technol. 210, 1203-1208.

[14] Remy, G., Jean-P., B., Georgette, R-P., Emilie, C., et al. ,2009. Separation of particles from hot gases using metallic foams, J. Mater. Process. Technol. 209, 3859-3868.

[15] Thilo, B., Joerg, B., Hans, W.B., 2001. Mechanical properties of structures of semifinished products joined to aluminum foams, J. Mater. Process. Technology. 115, 20-24.